Technical Evaluation Report
TAACOS: Target Acquisition with the TA1 Mirror

Date:	February 1, 2001
Document Number:	COS-11-0027
Revision:	Initial Release
Contract No.:	NAS5-98043
CDRL No.:	N/A

Prepared By: ______________________________ ________

S. Penton, COS Software Scientist, CU/CASA   Date

Reviewed By: ______________________________ ________

I. Becker, COS Software Consultant, BATC   Date

Reviewed By: ______________________________ ________

K. Brownsberger, COS Sr. Softwa Scie   ate

Approved By: ______________________________ ________

T. Keyes, Scientist, ST   Date

Approved By: ______________________________ ________

D. Ebbets, COS Software Con ant, B   Date

Approved By: ______________________________ ________

Jim Green, COS Principal Inv   Date

Approved By: ______________________________ ________

Erik Wilkinson, COS Scientist   Date

Approved By: ______________________________ ________

John Andrews, COS Experiment Manager   Date

Web-Released Document

Center for Astrophysics & Space Astronomy
University of Colorado
Campus Box 593
Boulder, Colorado 80309

REVISIONS

Letter	ECO No.	Description	Check	Approved	Date
-		Initial Release			

Original Release Name:	Date	
Drawn: S. Penton	2/1/2001	**THE UNIVERSITY OF COLORADO** At Boulder **The Center for Astrophysics and Space Astronomy**
Reviewed:		**Technical Evaluation Report** "TAACOS: Target Acquisition with the TA1 Mirror"
Approved:		

Size	Code Indent No.	Document No.	Rev
A		COS-11-0027	-
Scale: N/A			

TABLE OF CONTENTS

TABLE OF FIGURES

1. SCOPE

The purpose of the Target Acquisition Analysis for the Cosmic Origins Spectrograph (TAACOS, see COS-08-0011) is to ensure that the algorithms and procedures defined in COS OP-01, IN0090-619, IN0090-623 and COS-FSW-001 are sufficient to accurately place a science target of interest at a proper location in the aperture in a timely and efficient fashion. This document focuses solely upon our TAACOS simulations of target acquisitions (TA) with the TA1 mirror and the COS NUV channel. This topic was first addressed in COS-11-0024 (TAACOS: NUV Phase I Report). The TA1 discussion in COS-11-0024 has been expanded in this document. Further investigation into this topic has revealed additional operational complexities that have required us to modify our initial conceptualization of this TA mode. This document will outline our modifications for the LTAIMAGE TA mode, and introduce a new TA calibration lamp image mode (LTAIMCAL) which must be performed before each science target TA1 mirror TA (LTAIMAGE).

The COS TA requirement is that the science target should be aligned to within 45 km/s (~±0.24" for the NUV channel, ~±0.3" for the FUV channel, medium resolution) in the dispersion direction (DD) in the 3σ case for the medium resolution gratings. The NUV cross dispersion (XD) requirement is only that the target spectra should be fully contained in the predicted detector subarray used in spectral extraction. In the XD, target accuracies of ±0.5" (22 XD pixels) will ensure that no target flux is vignetted by the aperture. There exists an additional science requirement of allowing for TAs with DD accuracies of ±15 km/s (±0.08" for the NUV channel, ~±0.10" for the FUV channel, medium resolution) in the dispersion direction in the 3σ case for special observations. This equates to a DD centering accuracy of ~±3.5p.

Changes to our recommendations for the TA flight software (FSW), based upon this document, will be given in a revision (Rev A) of COS-11-0014. For further details of the TAACOS project, see COS-08-0011 or http://cos-arl.colorado.edu/TAACOS.

1.1 BACKGROUND

Although most HST/COS TAs are planned to be performed spectroscopically without the aid of sky images, there exists a COS mode which can produce broadband images suitable for TA. A flat mirror, TA1, can be rotated into the NUV optical path using the second (NUV) optical selection mechanism (OSM2). In this mode an image of the sky will be projected onto the NUV MAMA detector after reflection off the NCM3b mirror. This document details the proposed algorithms for this mode of TA.

The simulator and the analysis are performed using ray-tracing and other software developed using the Interactive Data Language (IDL) at CU/CASA. This effort relies heavily on ground-based estimations of the COS in-orbit performance. Final TA FSW algorithms will be tested during the integration and testing (I&T) phase of the COS development.

1.2 DOCUMENT OVERVIEW

In §2, we list the applicable COS documentation related to this report. In §3, we list the abbreviations and acronyms used in this document. In §4, we will briefly review the NUV MAMA detector, the coordinate systems used, the HST point spread function (PSF) at the COS science apertures, the input QSO spectrum, current estimates of the COS NUV effective areas and noise characteristics, intrinsic detector blurring, estimates of mechanism wobble and mis-alignment, and recommend LTAIMCAL and LTIMAGE TA extraction subarrays. Seasoned TAACOS veterans may wish to skip directly to §4.6 (MECHANISM WOBBLES AND EXTRACTION SUBARRAYS). In §5 and §6, we use our TAACOS NUV simulator to test the two imaging target acquisition (TA) phases, LTAIMCAL and LTAIMAGE. In §7, we briefly summarize our NUV imaging TA findings.

2. APPLICABLE DOCUMENTS

The following documentation describes the algorithms and procedures proposed for HST/COS target acquisition. The referenced documents are of the revision in effect on the date of the release of this document

COS-08-0011	TAACOS: Target Acquisition Analysis for the COS (CASA)
COS-11-0014 (Rev A)	Recommended Flight Software and Operations Changes based on the TAACOS Phase I Reports for the FUV and NUV Channels
COS-11-0016	TAACOS: FUV Phase I Report
COS-11-0017	TAACOS: Detector TA Summary FUV and NUV Images
COS-11-0024	TAACOS: NUV Phase I Report
COS-11-0028	TAACOS: OSM1 Positional Verification FSW
COS-FSW-001	Target Acquisition Concepts for COS (BATC)
COS-NUV-001	NUV MAMA Subsystem Performance
COS-SYS-022	Current Estimates of COS Sensitivity
COS-OP-01	COS Science Operations Requirement Document (CASA)
IN0090-619	Control Section Flight Software Requirements Document for the COS (BATC)
IN0090-623	Software Design Document for the Control Section Flight
ST-ICD-02E	Axial Scientific Instruments to Optical Telescope Assembly and Support Systems Module (STSCI)

3. LIST OF ACRONYMS AND ABBREVIATIONS

ACS	Aperture Coordinate System
BOA	Bright Object Aperture
BOP	Bright Object Protection
BR	detector Background count Rate
CASA	Center for Astrophysics and Space Astronomy
COS	Cosmic Origins Spectrograph
CU	University of Colorado @ Boulder
DD	Dispersion Direction (ACS X, IC Y)
DCS	Detector Coordinate System
FOS	Faint Object Spectrograph
FSW	Flight SoftWare
FUV	Far UltraViolet
FWHM	Full Width at Half Maximum
GSC2	Guide Star Catalog II
HST	Hubble Space Telescope
IC	Image Coordinate system
IDL	Interactive Data Language
I&T	Integration and Testing
LTAIMCAL	TA subroutine for IMaging the CALibration lamp
LTAIMAGE	TA subroutine for target Locating with the TA1 mirror
LTASRCH	TA subroutine to Locate the target via a spiral SeaRCH
MAMA	Multi-Anode Microchannel Array
MBPFC	Moving Box Plus Flux-Centroid (STIS) algorithm
NUV	Near UltraViolet
OSM	Optical Select Mechanism
p	Pixel
PSF	Point Spread Function (of HST)
PtNe	Platinum-Neon (Wavelength Calibration Lamp)
PSA	Primary Science Aperture
QSO	Quasi-Stellar Object
RVMM	Rear View Mirror Mode (TA1)
s	second
STIS	Space Telescope Imaging Spectrograph
SR	Source (target) count Rate
TA	Target Acquisition
TA1	Target Acquisition 1 (one) mirror
TAACOS	TA Analysis for COS
TS	(Spiral) Target Search
XD	Cross-Dispersion (ACS Y, IC X) direction

4. NUV DETECTOR OVERVIEW AND PERFORMANCE ANALYSIS

4.1 BACKGROUND AND THE NUV DETECTOR COORDINATE SYSTEM

The COS NUV detector is the STIS flight spare band 2 MAMA. The detector is illuminated by three independent camera mirrors, which are part of the NUV optical path (see COS-11-0001). Each of the three mirrors produces a spectral stripe on the detector. Each of the MAMAs 1024x1024 pixels are 25µm on a side. Figure 1 displays the COS MAMA detector coordinate system (DCS), and shows the location of the three science and wavelength calibration stripes. Unlike the FUV DCS, the NUV dispersion direction (DD) is identified as Y and the cross-dispersion (XD) direction is X.

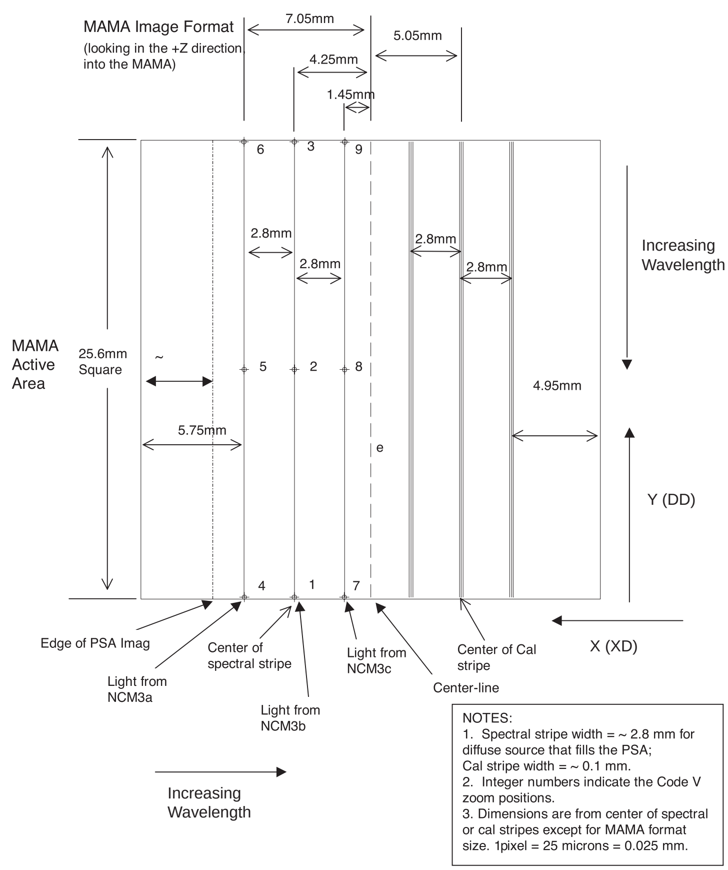

Figure 1: NUV Detector Coordinate System. This figure details the physical locations of the three science and wavelength calibration NUV spectral stripes. This figure was taken from COS-11-0001.

4.2 THE HST POINT SPREAD FUNCTION AND COS SCIENCE APERTURES

As pointed out in the COS-11-0016, a primary driver to the COS TA algorithms is the relationship between the size of the point spread function (PSF) of HST and the COS aperture at the aperture location. The on-axis unfocused HST PSF is approximately symmetric with a radius of ~0.204mm (0.75”). Figure 2 displays the HST PSF of a point source at the COS primary science aperture (PSA) in coordinates of millimeters and arcseconds on the sky. The 2.5” diameter aperture is shown in red, simulated photons from an isolated point source are shown in green. The hashed area indicates the aperture mechanism, which blocks photons not in the aperture. The PSA and the bright object aperture (BOA) are both 0.340mm (1.250”) in radius. Therefore, the COS science apertures capture 100% of the HST PSF, plus an additional ~0.136mm (0.5”) annulus (indicated by Δr in Figure 2). We define the aperture coordinate system (ACS) as having X in the horizontal direction and Y in the vertical of Figure 2. In our ACS, the origin is at the center of the aperture with X increasing to the right and Y increasing upward when looking forward in HST bay 4. In our analysis we will be comparing initial HST pointings in the dispersion direction (DD, X_0) and in the cross-dispersion direction (XD, Y_0) to the final telescope pointings (X_f and Y_f). We will commonly compare the mean of the absolute value of the pointing errors. We designate this as $\langle|X_f\text{-}X_0|\rangle$ in the DD and $\langle|Y_f\text{-}Y_0|\rangle$ in the XD. Owing the rotation of the detector coordinate system (DCS) to the ACS, ACS X and DCS Y are in the DD, while ACS Y and DCS X are in the XD. In this document, X_0, Y_0, X_f, and Y_f will always refer to ACS coordinates.

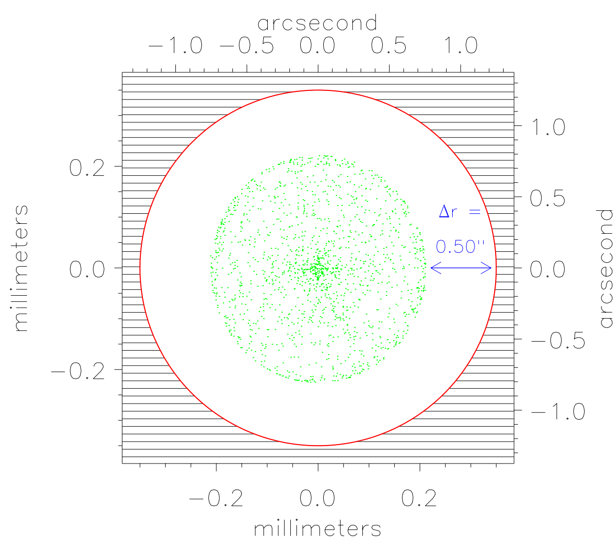

Figure 2: The HST PSF as compared to the COS PSA. The aberrated, out of focus, HST PSF is approximately circular with a radius of ~0.2 mm at the COS aperture mechanism. The COS PSA is circular with a radius of 0.34mm, which corresponds to 1.25” on the sky. The HST PSF is smaller in radius than the COS PSA aperture by 0.136mm or ~0.5”.

4.3 TAACOS: INPUT SPECTRUM

As with previous TAACOS simulations, our input spectrum is based upon the faint object spectrograph (FOS) QSO composite spectrum (Zheng, et al. 1998, ApJ, 492, 855). The TAACOS NUV input spectrum used in this analysis differs from the FOS QSO composite spectrum in the following ways:

1) It has been scaled to an average flux level of $F_\lambda = 10^{-14}$ ergs/cm^2/s/Å.This is 10 times brighter than the TAACOS FUV target.
2) It has been adjusted to correspond to a target with z=0.125.
3) OI λ2471 Geocoronal emission has been added. TAACOS analysis, based upon STIS in-orbit measurements of the strength of the OI λ2471, indicate that this weak emission line should not affect NUV TA. Therefore, unlike the FUV channel, no special TA subarrays are necessary to mask out this Geocoronal feature during NUV TA.
4) Simulated non-physical absorption features are inserted into the spectrum at regular intervals ranging from equivalent widths of 2 Å to 2 mÅ. These spectral features are a convenient method for determining the sensitivity limits of COS observations.

Figures 4-6 of COS-11-0016 display the input spectra for the FUV detectors, without Geocoronal lines. The TAACOS NUV spectra are similar, but at higher wavelengths.

4.4 COS EFFICIENCES AND DETECTOR NOISE

The COS instrument (optics + detectors) efficiencies used for the NUV TA with theTA1 mirror analysis are taken from (COS-SYS-022) and are current as of January 27, 2000. For convenience, these efficiency results are presented in Figure 3. For purposes of TA, we assume that the detectors will have a constant background rate of 34 counts s^{-1} cm^{-2}. This rate is based upon the in-flight count rate currently being detected by the STIS flight MAMA, corrected for background count rate differences between the nearly identical MAMAs. This count rate equates to 223 counts s^{-1} over the entire detector or about one count per pixel every 78 minutes. This background rate is a factor of 70 higher than the FUV background rate and has important implications regarding NUV TA.

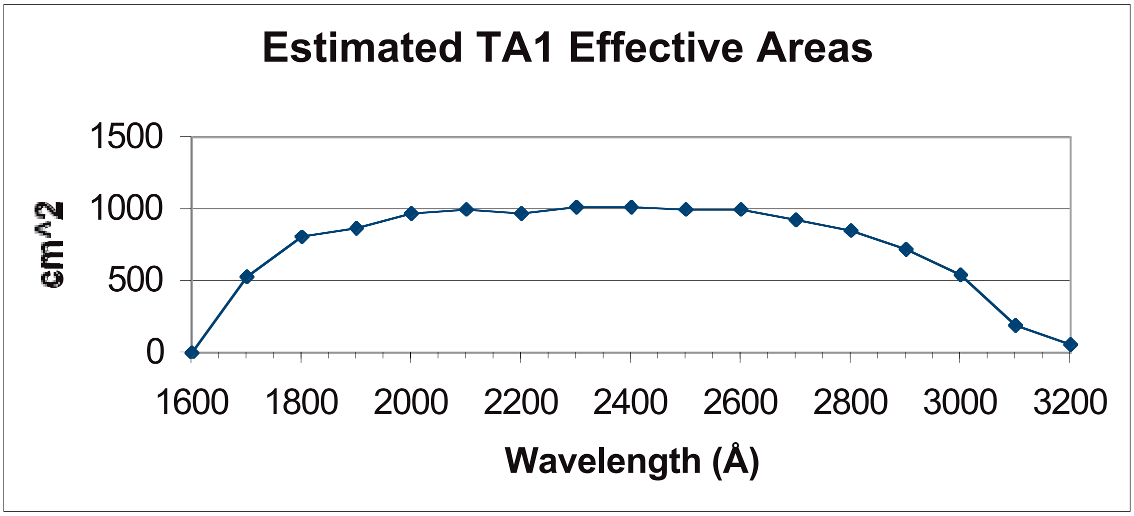

Figure 3: HST+COS NUV TA1 effective areas (in cm^2) as a function of wavelength. This figure was taken from COS-SYS-022.

4.5 DETECTOR BLURRING

The NUV detectors produce charge clouds that are unique to each incoming photon energy and microchannel plate location. However, this also means that photons of the same energy and location will produce different cloud charges and detector locations. As such, no readout electronics can detect the incoming photon's physical location to better than this intrinsic "blurring". For the COS NUV detectors, the radial blurring is ~32µm FWHM (full width at half-maximum) in both the DD and XD (COS-NUV-001). This intrinsic blurring is added to each incoming photon to create an image of the NUV detector in physical space.

4.6 MECHANISM WOBBLES AND EXTRACTION SUBARRAYS

The OSM mechanisms have known mechanical imperfections that cause slight mis-alignments in both the dispersion (DD, IC Y) and cross-dispersion (XD, IC X) directions. Since the imaging modes described in this document use undispersed light, will we primarily refer to the IC X and Y coordinates. These errors can be divided into two categories, wobble and step errors. Step errors refer to situations where the OSM mechanisms do not achieve the desired rotational positions. These errors cause Y offsets only. A 1 step OSM1 error equates to an image offset of ~±240 pixels (p), while an OSM2 1 step error equates to a ~±50p offset. Wobble refers to motion isolated to the grating or mirrors being employed. Wobble occurs in both the X and Y direction. Simulations indicate that the maximum wobble introduced by OSM1 and OSM2 at the MAMA is expected to be ~±30p in Y and ~±80p in X. In addition, the calibration image has a certain intrinsic spatial extent, which must be accounted for. We estimate that allowing an additional ±20p should be sufficient for the calibration lamp image. Therefore, to be reasonably certain that we have allowed for mechanism 'slop' we need to allow for the following possible alignments errors:

Y allowance = ± (240+50+30+20)p = ±340p
X allowance = ± (80+20)p = ±100p

TAACOS simulations indicate that in the absence of mechanism mis-alignments, the center of the calibration image (the calibration lamp imaged with OSM2 set to the TA1 mirror) should fall at IC (X, Y) coordinates of ~(286,471). Therefore, to ensure that the calibration lamp image is recovered, the extraction subarray should be from IC coordinates (186,131) (lower right) to (386,811) upper left. When considering target acquisition, one must allow for target misalignments within the aperture. The largest initial pointing error which will still produce target counts is the aperture radius plus the PSF radius, or ~2'' (arcseconds). Since this is the maximum possible extent, no spatial dimension allowance is necessary for point sources TAs. TAACOS simulations (COS-11-0024) indicate that when the TA1 mirror is in the optical path, the detector plate scales are:

-42.554 ± 0.004 p/" (IC X vs. Aperture Y")
-42.469 ± 0.003 p/" (IC Y vs. Aperture X").

This equates to an additional ±2" allowance of ~± 85p for astronomical targets. TAACOS simulations indicate that a perfectly centered target, with no mechanism misalignments, falls at IC coordinates of ~(678,531). Therefore, to ensure that the target image is recovered, the extraction subarray should be from IC coordinates (513,126) (lower right) to (843,936) upper left. These subarrays are displayed in Figure 4. These subarrays are only initial estimates for the current TA1 mirror alignment. Plans are underway to slightly tilt the TA1 mirror to move the central target and calibration images off of spectral stripe 'B' (between stripes 'B' and 'C'). In addition, when using the 'rear view mirror mode' (RVMM), it is planned to center the target and calibration images between stripes 'A' and 'B'. Also shown in Figure 4 are simulated target and calibration images, along with background estimates.

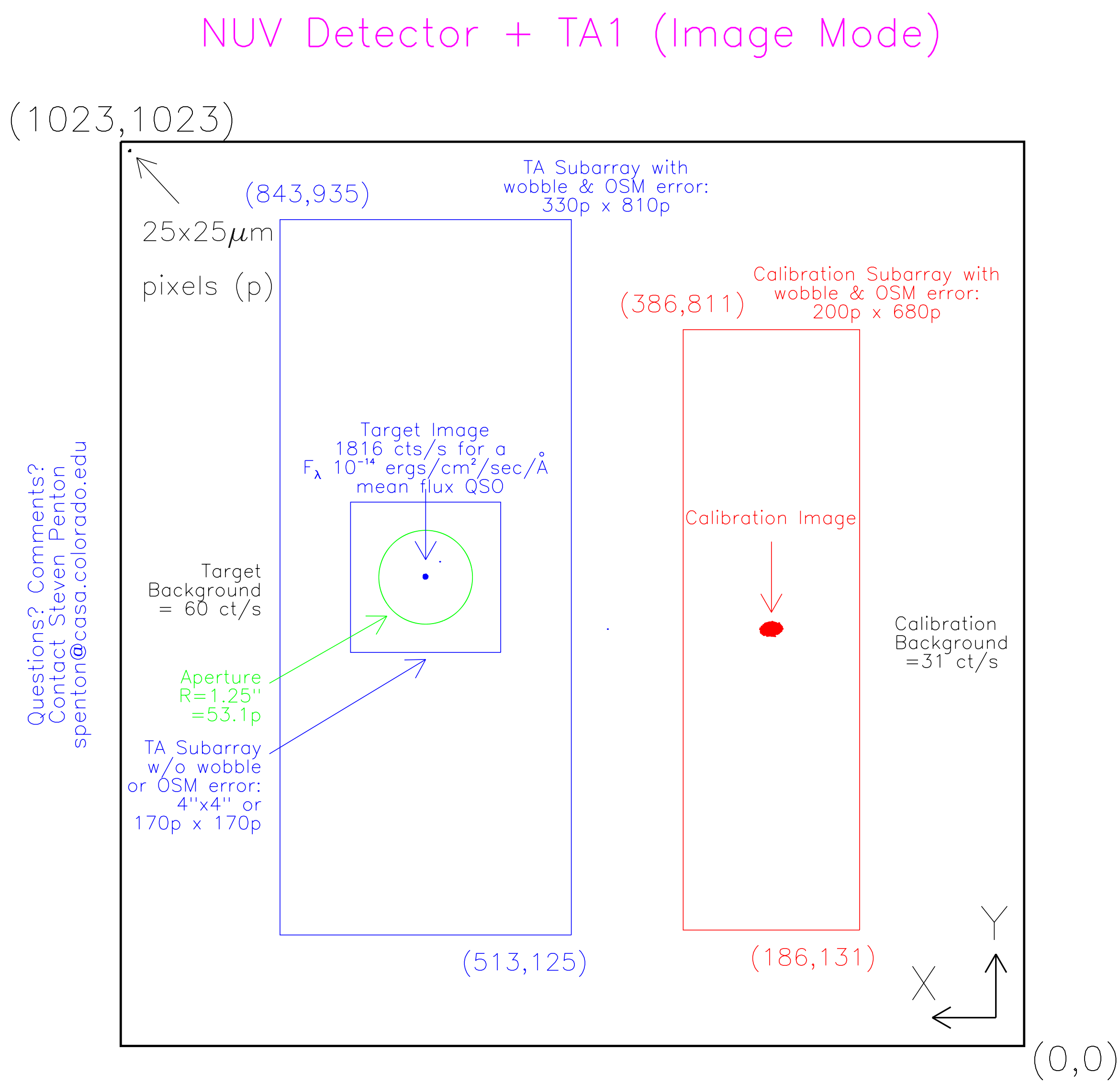

Figure 4: TA1 extraction subarray summary. The LTAIMCAL and LTAIMAGE extraction subarrays are compared in IC to simulated images and the COS science aperture. Expected MAMA background rates are also given.

5. LTAIMCAL

5.1 INTRODUCTION

Due to possible mechanical mis-alignments, it is necessary to flash the calibration lamp, with OSM2 rotated to the TA1 mirror, to determine the position on the detector corresponding to the center of the calibration, and thus the science, aperture(s). This (new) TA phase is referred to LTAIMCAL. The extraction subarray for this TA phase was given in the previous section. In this section, we examine various options for determining the center of the rectangular calibration aperture. Once this location is determined, a known offset is applied (via patchable constants) to calculate the detector location corresponding to the center of the science aperture.

5.2 ANALYSIS

We considered the following four algorithms for determining the center of the calibration aperture from a calibration lamp ACCUM or TIME-TAG image:

1) Use the mean X and Y TIME-TAG event location to determine the X and Y centroids of the calibration lamp image.

2) Use the median X and Y TIME-TAG event location to determine the X and Y centroids of the calibration lamp image.

3) Construct 2–1D histograms of the TIME-TAG event locations (1 histogram each for the X and Y event locations). Use the histogram bin with the maximum counts to determine the X and Y centroids of the calibration lamp image. If multiple bins have the same counts, use the first bin encountered.

4) Obtain an ACCUM image of the calibration lamp. Following the algorithm used with HST+STIS, move an 11x11p box across all possible box locations to determine the 11x11p region of the image (histogram) that contains the most events. Use a flux-centroid algorithm on this 11x11p box to determine the X and Y centroids of the calibration lamp image.

The spatial extent of the calibration image is shown in Figure 4. Figure 5 displays a TAACOS simulation of the undispersed wavelength calibration lamp in IC. Background noise has not been included in this simulation since the actual exposure time of the LTAIMCAL exposure has not been determined at this point. The exposure time, and hence the detector background rate, is the most important determining factor in choosing an LTAIMCAL centroid algorithm. The X asymmetry of the calibration image is of marginal concern since this is the cross-dispersion (XD) direction. In Figure 6 we compare simulated centroiding accuracies for the four algorithms tested. The **maximum** wobble plus mechanism rotation error (1 step) was assumed. We find that as long as the

LTAIMCAL exposure time is less than 10 second (which is extremely probable), the median algorithm is more than sufficient for X and Y centroiding. Errors in LTAIMCAL centroiding should introduce less than or approximately equal to a ±0.01” error in predicting the location of the science aperture center in both X and Y. Following the timing assumptions of COS-11-0024, this phase should take approximately 30 seconds (allotting 10 seconds each for BOP check, lamp exposure, and software overhead.

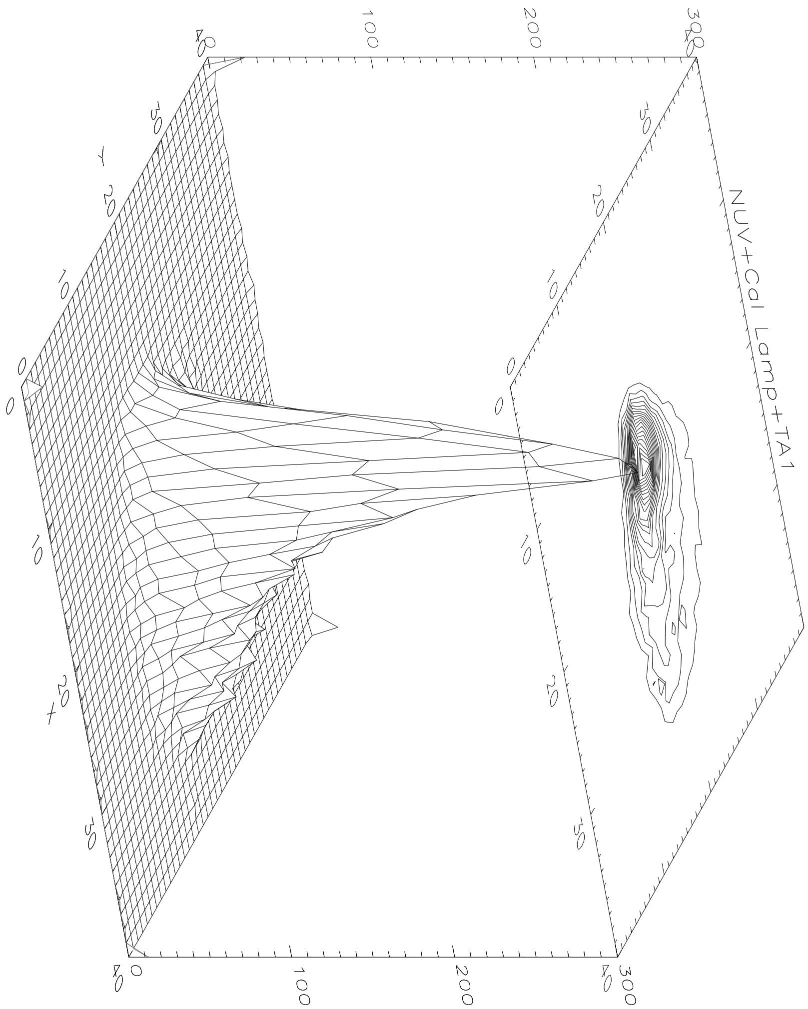

Figure 5: TAACOS-simulated NUV TA1 calibration lamp image shown in instrument coordinates (IC). X and Y IC are 25x25µm pixels. The Z-axis is in units of counts.

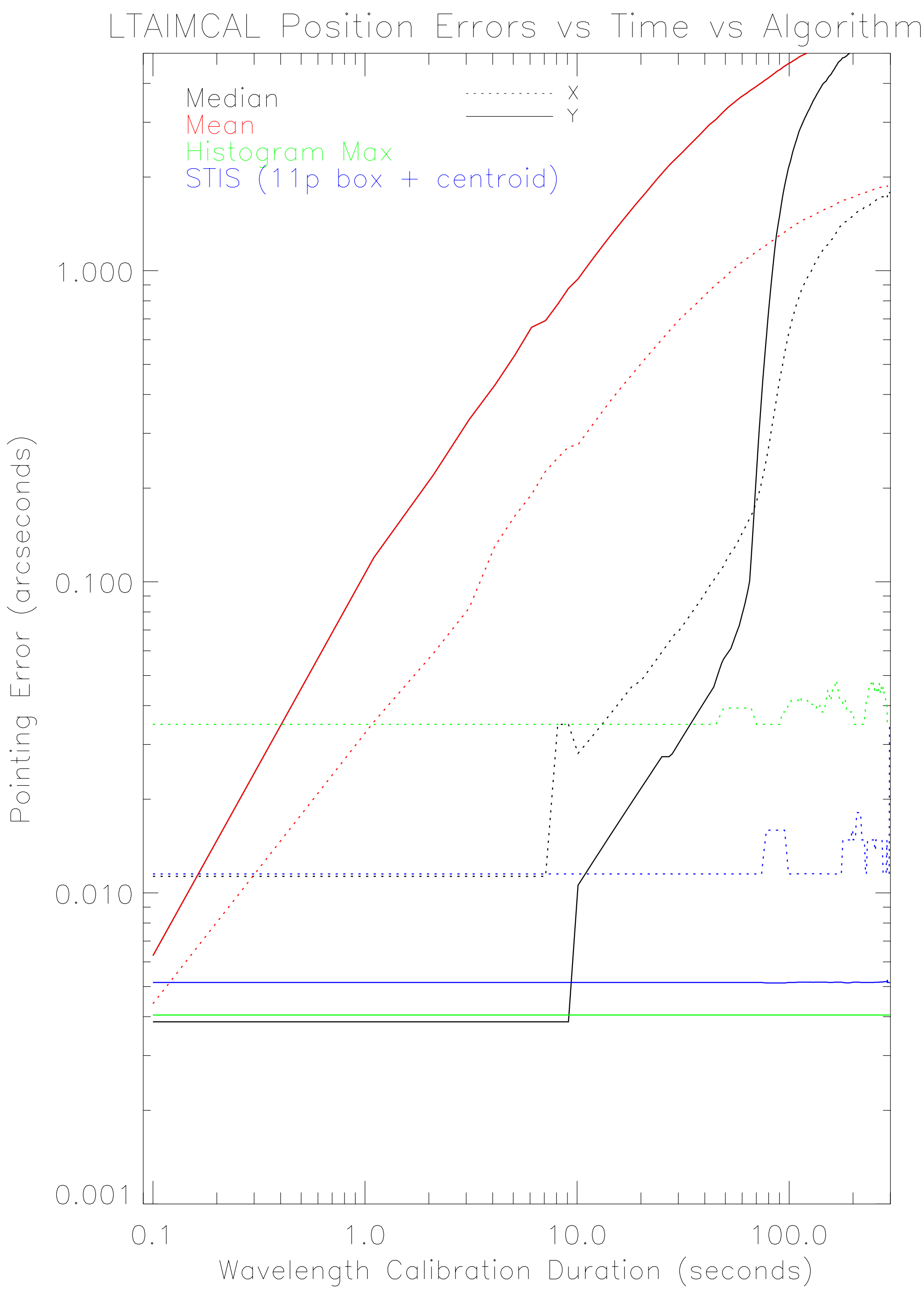

Figure 6: Predicted maximum LTAIMCAL centroid calculation errors (in arcseconds) as a function of exposure time and LTAIMCAL centroiding algorithm.

5.3 OSM1 MECHANISM ADJUSTMENT

There exists a science requirement (COS-OP-01) that the central wavelength of a science acquisition places a pre-selected wavelength at the center of a spectral stripe to within ± 50 spectral resolution elements in the dispersion direction (DD, Y). For the NUV channel, this corresponds to placing the target image during LTAIMAGE to within ~ ± 150 pixels in the Y direction of the perfectly aligned location. In instruments coordinates (IC), TAACOS simulations indicate that this location is (678.4,530.8) [X, Y; pixels]. However, as pointed out in §4.6, the various mechanism foibles can contribute to Y (DD) mechanism alignment. Specifically, the predicted mechanism induced Y (DD) coordinate mis-alignment contributors are:

- OSM1 + OSM2 'wobble' = ± 30p
- 1-step OSM1 rotation error = ± 240p
- 1-step OSM2 rotation error = ± 50p

Clearly, the major contributor is the 1-step OSM1 rotation error. The LTAIMCAL procedure can be used to help eliminate this error. This is discussed in COS-11-0028. TAACOS simulations indicate that, in IC, the position of the properly aligned calibration image is at (286.5,471.2) [X, Y; pixels].

The specific LTAIMCAL steps are outlined in COS-11-0014 (Rev A).

6. LTAIMAGE: TARGET ACQUISITION USING THE TA1 MIRROR

6.1 INTRODUCTION

TA using an image of the sky is possible with COS using the TA1 mirror on OSM2 to image the sky on the MAMA. We call this operation LTAIMAGE. This operation is theoretically limited to sources within a 2" radius (85p) of the center of the aperture. This maximum distance, 2", is the distance from the center of the aperture where photons reach the detector (1.25" radius aperture + 0.75" radius PSF). Operationally, LTAIMAGE works well out to initial radial offsets of up to 1.7". As previously pointed out, wobble and rotation errors in the OSMs cause the detector location of a target centered in a science aperture to vary with exposure.

The use of this procedure requires that the initial HST slew places the object within 1.7" of the center of the aperture. This should be possible for many targets when the GSC II is available. Target with additional positional uncertainties may require a spiral search (LTASRCH) be performed before LTAIMCAL+LTAIMAGE.

To determine the detector location of a target centered in the aperture, two pieces of information are required. These are:

1) The X and Y centroids of the TA1 mirror calibration lamp image with the OSMs in the science exposure positions. This information is provided by the LTAIMCAL TA phase.

2) The offset between the centroid of the calibration aperture and the science aperture. This information will be determined on the ground and used by LTAIMAGE to calculate the detector location of a point source centered in the aperture.

In addition to the X and Y detector coordinates of a centered external point source, two additional pieces of information are required. These are:

1) The plate scales, the relationships between arcseconds (“) on the sky and X/Y pixels (p) on the detector. These have been simulated by TAACOS and will be tested on the ground, and possibly verified in flight.

2) The X and Y centroids of an image of the sky containing the target source taken with OSM2 rotated to the TA1 mirror.

Once this information is known, the centering of the target in the aperture involves the simple calculation, and implementation, of the desired HST slew. In this section, we examine different methods for determining the X and Y centroids of the target image. Recall that the actual location of the target image can cover a large region of the detector. The background count rate over this large extraction subarray (derived in §4.6) is predicted to be ~60 counts/second.

6.2 ANALYSIS

We tested 6 methods for calculating the X and Y centroids of the LTAIMAGE. These methods are divided into two classes. The first class uses the entire extraction subarray derived in §4.6, while the second class uses the calculated detector coordinates of the LTAIMCAL phase and a smaller extraction box which represents the extent of the aperture on the sky (±2”, 170x170p). The latter methods are referred to as “small box” methods. The small box methods substantially decrease the predicted background contamination and serve as mild protection against detector “hot spots” which have not been included in these simulations nor excluded by the tested algorithms. The LTAIMAGE centroiding methods considered were:

1) Use the mean X and Y TIME-TAG event locations over the extraction subarray to determine the X and Y centroids of the target point source image.

2) Use the median X and Y TIME-TAG event locations over the extraction subarray to determine the X and Y centroids of the target image.

3) Same as 2), but using the small extraction box (conceptually, this algorithm +LTAIMCAL is the exact 2D analogy of the 1D LTACAL+LTAPKXD spectroscopic algorithm).

4) Construct 2 –1D histograms of the TIME-TAG event locations (1 histogram for the X event locations, 1 histogram for the Y event locations) over the entire extraction subarray. Use the histogram bin with the maximum counts to define the X and Y centroids of the target image. If two bins have the same counts, use the first bin encountered.

5) Same as 4), but using the small extraction box.

6) Obtain an ACCUM image of the calibration lamp, or construct 1–2D histogram of the TIME-TAG event locations. Following the algorithm used with HST+STIS, move a 9x9p box across all possible box locations to determine the 9x9p region of the image (histogram) that contains the most events. Use a flux-centroid algorithm on this 9x9p box to determine the X and Y centroids of the target image. (A STIS-like "small box" method was not considered since it was assumed that this would not affect the determination of the maximum count box.) It should be noted that a flux-centroid image algorithm is mathematically equivalent to a mean TIME-TAG event list centroid. We will refer to this mode as the STIS or Moving Box Plus Flux Centroid (MBPFC) method.

Figure 7 displays our TAACOS simulated Y (DD) centroiding error as a function of mean QSO target flux over the range of 10^{-18} ergs/cm^2/s/Å < F_λ< 10^{-13} ergs/cm^2/s/Å. Each exposure was performed for an exposure time that achieved ~500 total target counts (1 second for a F_λ=10^{-14} ergs/cm^2/s/Å source). For these simulations, the target was displaced from the aperture center by 1" in both ACS X and Y. In addition, the **maximum** wobble plus mechanism rotation error (1 step) was assumed. A pointing error of +0.01" based upon the LTAIMCAL simulations is included in the reported pointing accuracies. Figure 8 displays the predicted X (XD) centroiding errors. As expected, in all cases the "small box" methods achieved better centroiding accuracies to lower target flux values. Three methods, the full and small box, 2-1D histogram-maximum methods and the STIS-like box methods achieved our DD desired accuracies of < 0.08" in the DD (Y) down to a mean target flux F_λ=10^{-17} ergs/cm^2/s/Å. Below F_λ=10^{-17} ergs/cm^2/s/Å, only the STIS-like and small box histogram-maximum methods achieved the desired centering accuracies. These three methods also achieved our XD required accuracies.

Figure 9 displays a 1 second TA1 image for two F_λ=10^{-14} ergs/cm^2/s/Å QSO sources separated by 1" in both ACS X and Y. The stronger (rear) detection is perfectly centered in the aperture. The weaker feature is partially vignetted by the aperture, yet retains a narrow, circular, profile. This reassures us that our centroiding accuracy is independent of initial target position within the central 1" radius of the aperture center.

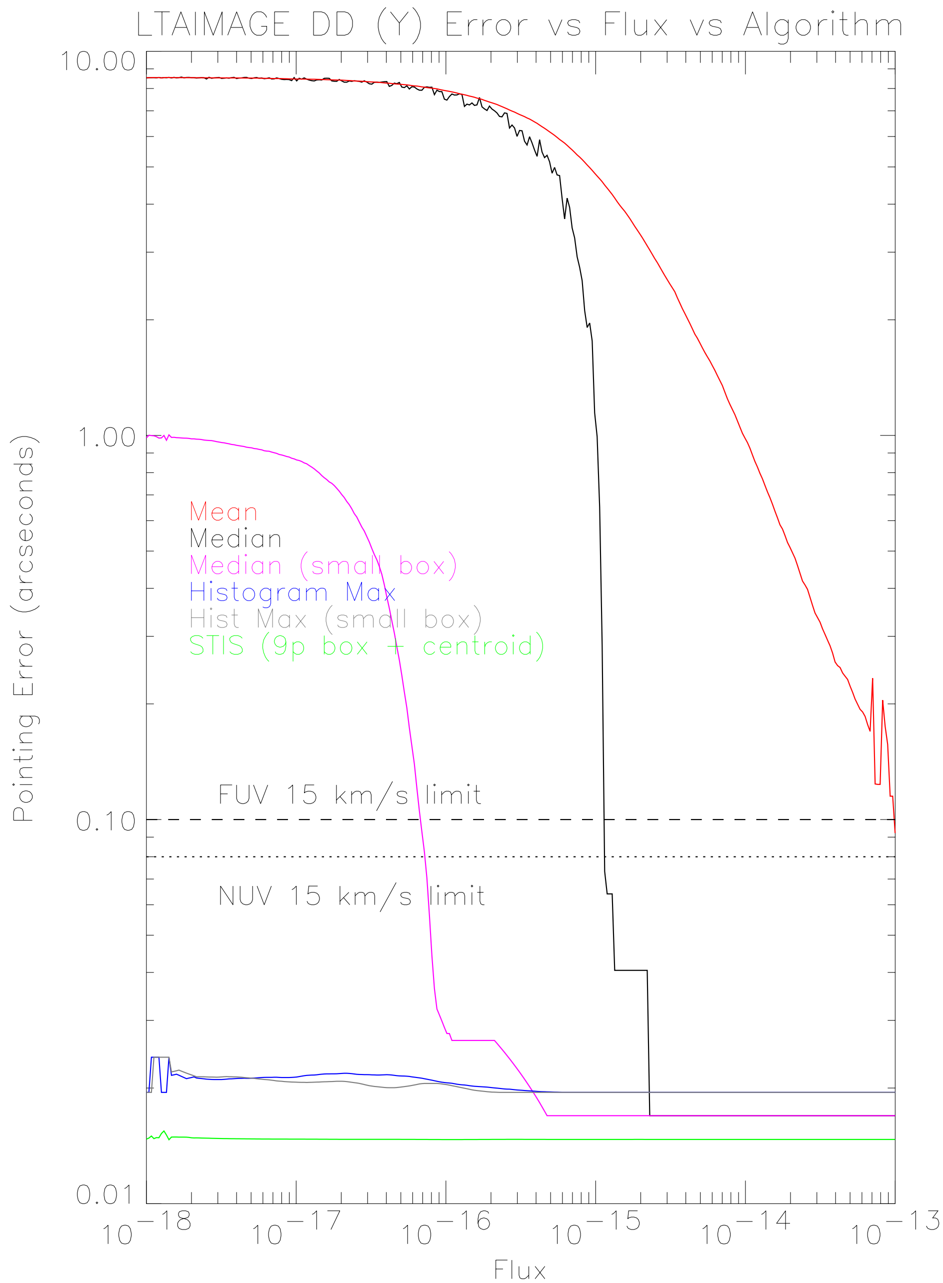

Figure 7: Dispersion Direction (DD, Y) pointing accuracy comparison of the tested LTIMAGE algorithms versus mean target flux for an extreme mis-alignment. The final pointing error (in arcseconds) includes a +0.01" LTAIMCAL allowance. The dashed lines indicate the 15 km/s DD FUV and NUV desired accuracies.

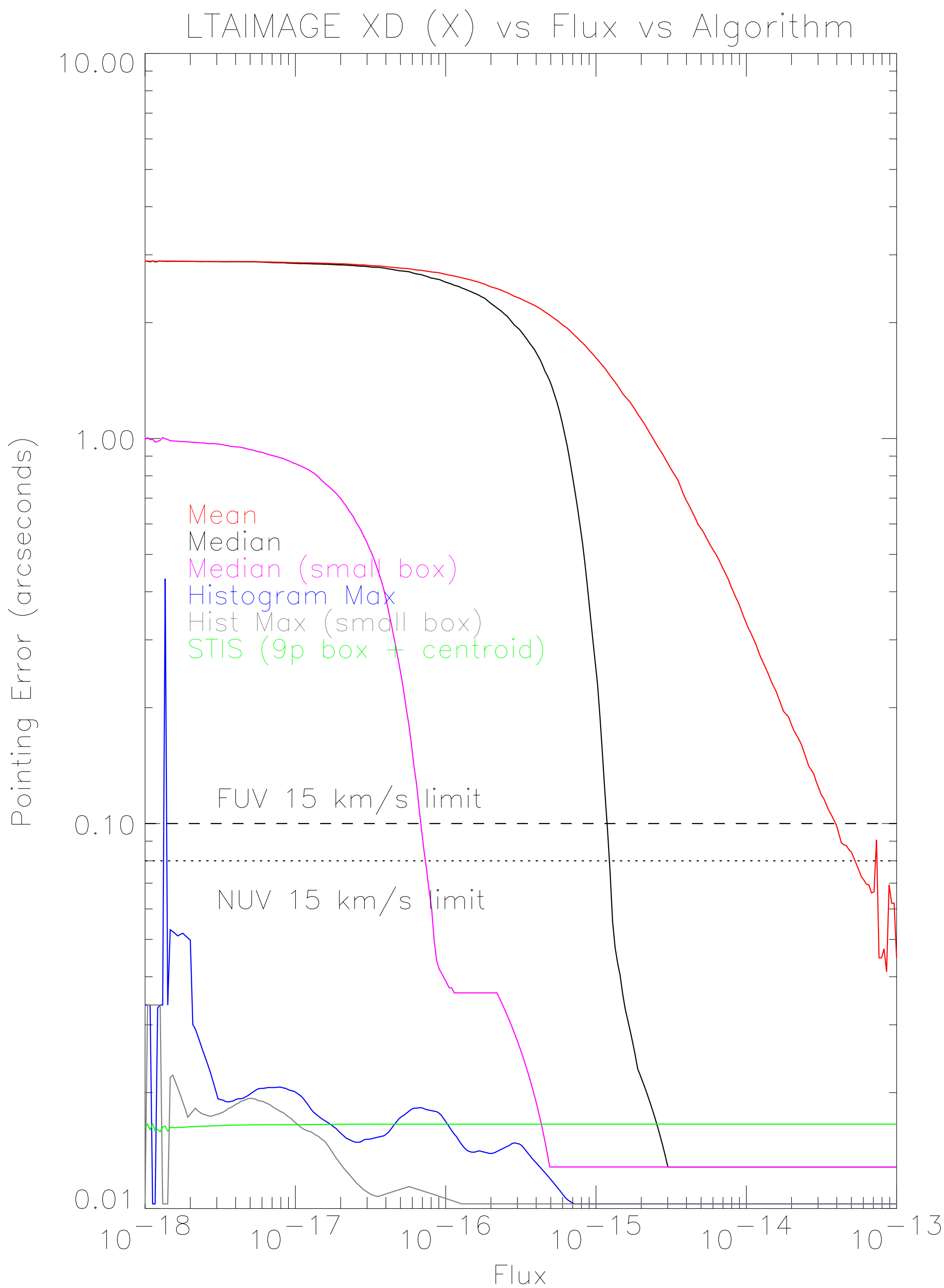

Figure 8: Cross Dispersion direction (XD, Y) pointing accuracy comparison of the tested LTIMAGE algorithms versus mean target flux for an extreme mis-alignment. The final pointing error (in arcseconds) includes a +0.01" LTAIMCAL allowance. For comparison, the dashed lines indicate the 15 km/s DD FUV and NUV desired accuracies.

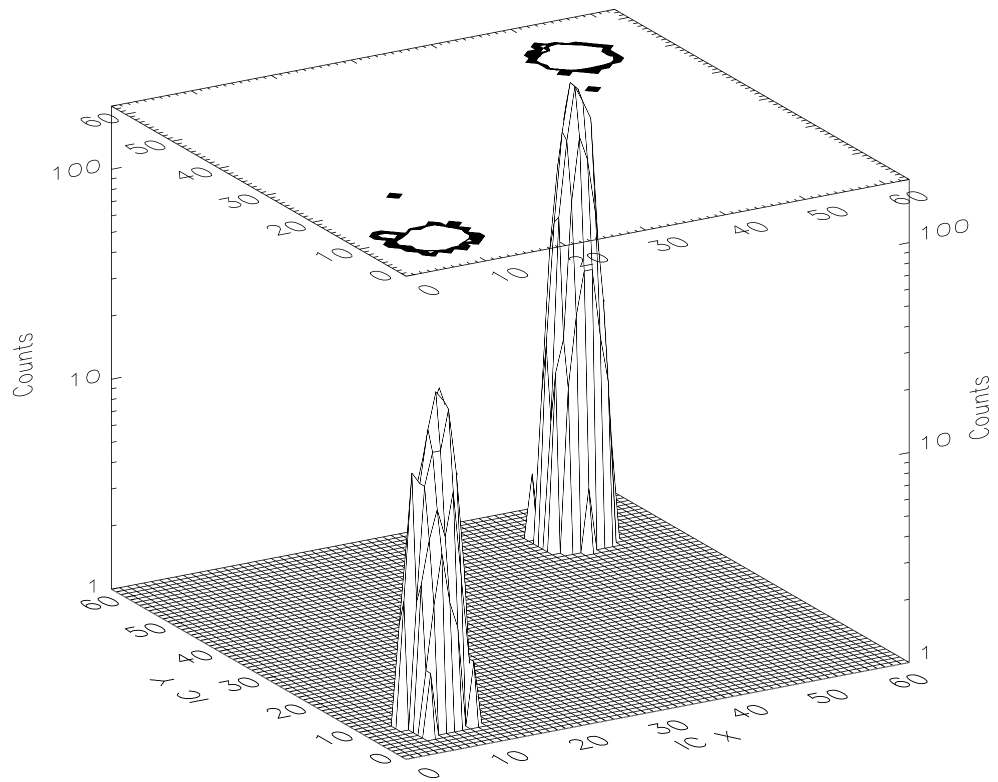

Figure 9: TA1 image of two point sources. The stronger one is centered in the aperture, while the weaker one is offset 1" in both ACS X and Y, and is partially vignetted.

6.3 LTAIMAGE EXPOSURE TIMES

A major concern when using this non-dispersed mode is the overillumination of the NUV MAMA. There exist two count rate restrictions for the NUV. One is a global limit of 10^6 counts/s over the entire detector. The other, local, limit is 200 counts/s/p. The central pixel of a TA1 image of our sample QSO spectrum achieves this count rate at the mean flux level of approximately F_λ=1.3x10^{-14} ergs/cm^2/s/Å. Because of the uncertain flux and variability of astrophysical targets, the exposure times used for LTAIMAGE should be conservative. As such, we adopt a stricter local limit 100 counts/s/p in our analysis; however, this count rate is probably still too large. For targets brighter than F_λ=1.3x10^{-14} ergs/cm^2/s/Å, two methods of flux attenuation are possible. The first is to position the target in the BOA This aperture has a neutral density filter that attenuates flux by a factor of 100. Alternately, the RVMM of the TA1 mirror can be used (COS-OP-0001). This mode also attenuates flux by about a factor of 25. Because it does not involve routine motion of the aperture mechanism, it is assumed that targets above a certain count rate will be attenuated with the RVMM, while targets brighter could be attenuated with both the BOA and RVMM. Figure 10 displays estimated maximum count rates for the brightest pixel in the TA1 image for mean fluxes in the range of F_λ=10^{-17}-10^{-11} ergs/cm^2/s/Å, assuming a maximum local count rate limit of 100 counts/s/p. The green line indicates the maximum count rates for un-attenuated observations. Fluxes exceeding 100 counts/s (dashed green line) are attenuated with the RVMM (display in red), while fluxes that exceed the count rate limit by a factor of 25 are attenuated by the BOA (blue). Fluxes that exceed the count rate limit by a factor of 250 are attenuated by both the BOA and RVMM (displayed in magenta). Sources with mean F_λ > ~6 x 10^{-11} ergs/cm^2/s/Å would not be observable with the TA1 mirror.

The local count rate limit has serious consequences on the S/N of the TA1 image. The S/N of a NUV+TA1 image can be calculated by Equation 2 of COS-11-0024. The background count rate (BR) for a 170px170p extraction should be ~7 counts/s, and 0.03 counts/s for an 11x11 extraction box typical of the MBPFC method. In Figure 11, we display the exposure times required to achieve a S/N of 10 in the brightest pixel for both the small-box (170x170p) histogram-max and the moving-box (11x11p box)+flux-centroid LTAIMAGE methods for the obtainable flux range. A maximum local count rate of 100 counts/s/p is assumed. Exposure times in green are un-attenuated; those in red, blue, and magenta have been attenuated by the RVMM, BOA and BOA+RVMM, respectively.

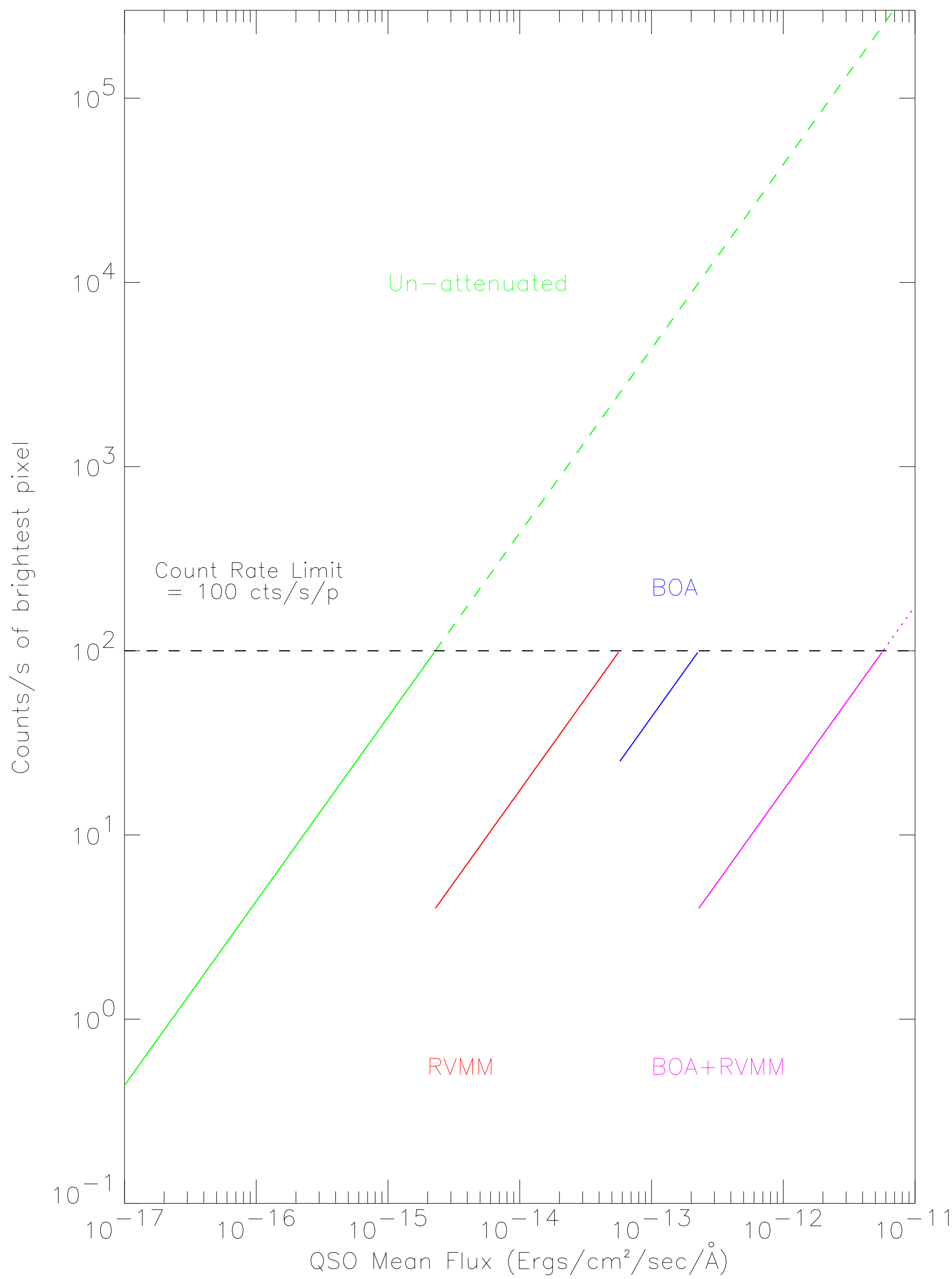

Figure 10: Count rate of brightest pixel vs. mean QSO target flux for NUV TA1 images. The solid curves are for un-attenuated, the 'rear view mirror mode' (RVMM), the bright object aperture (BOA) mode, and the combined BOA+RVMM.

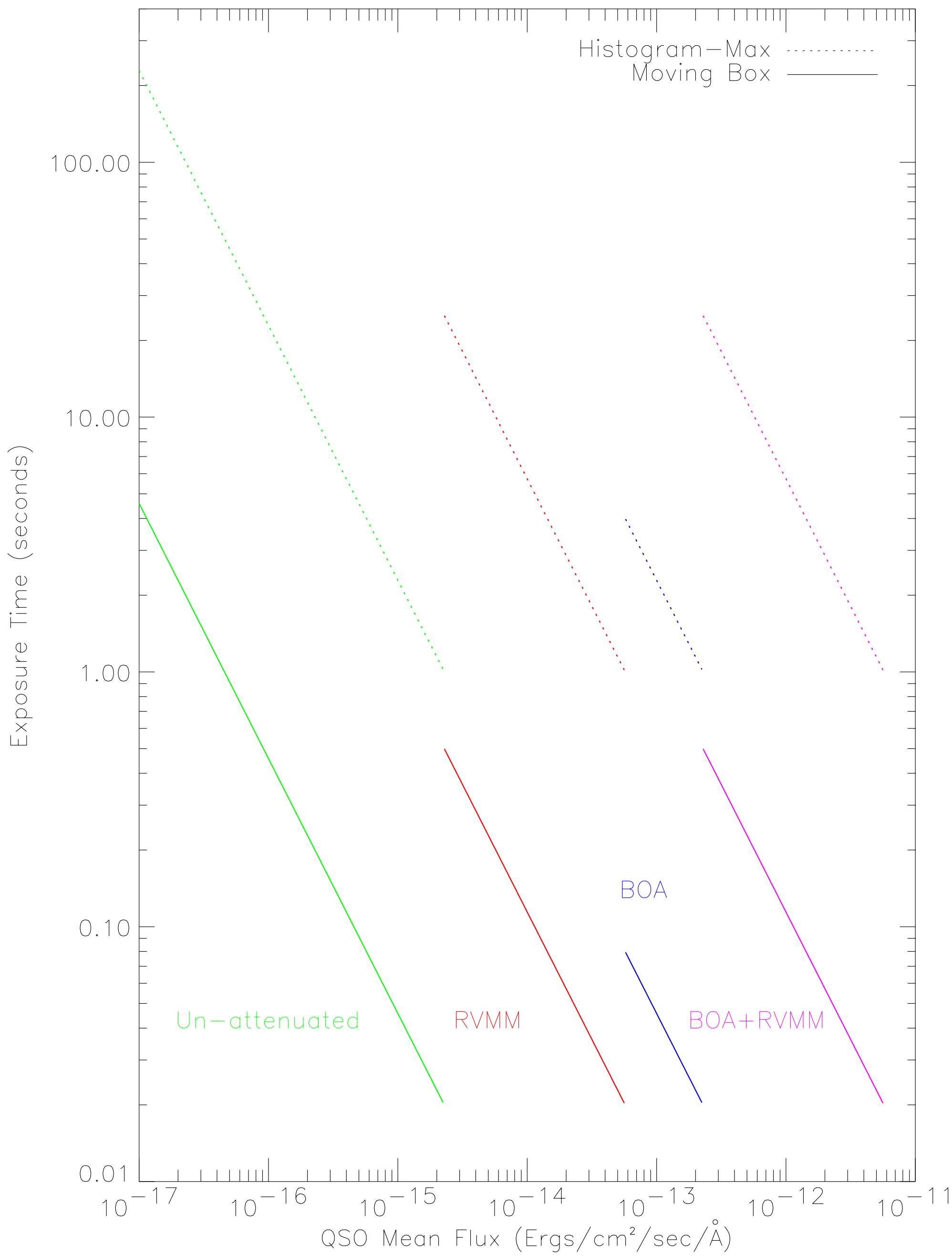

Figure 11: LTAIMAGE exposure times required to reach S/N ratios of 10 in the brightest pixel/histogram bin versus mean target flux. The histogram-max algorithm times are computed for a 170x170p box, while the MBPFC times assume an 11x11p moving box.

6.4 LTAIMAGE TIMING

Assuming that the external shutter is open, and the NUV detector is in the HVNOM state, a LTAIMAGE should take:

BOP Check	10s
LTAIMAGE Exposure	0.01-200s
LTAIMAGE slew	40s
OSM2 rotation	120s
LTAIMAGE software execution	5-180s (depending on algorithm)
Total	175-550s (2-10m)

LTAIMAGE searches could take anywhere from 176s up to ~500s, depending on the flux of the target, the S/N of the observation and the centering algorithm (histogram-max or flux-centroid). For most applications, the LTAIMAGE exposure time would average about < 100s. Using this exposure time, a typical LTAIMAGE exposure would take <275s. Our estimate of 120s for an OSM2 rotation is the maximum allowable as described in COS-SYS-012 Rev A (Optics Select Mechanism 2 Requirements). Our estimate of 180s for the maximum software execution time pertains to the MBPFC method. If a post-TA image were desired this would require approximately 2 minutes.

7. SUMMARY

We find that the proposed two-stage LTAIMCAL+LTIMAGE procedures are adequate for performing imaging TA using the TA1 mirror on OSM 2 in conjunction with the NUV MAMA. For the LTAIMCAL mode, using a median algorithm on a TIME-TAG event list should provide knowledge of the detector location of the aperture center to within ±0.01”. Absolute knowledge of the relationship between the flat-field and science apertures was assumed. TAACOS simulations indicate that three LTAIMAGE algorithms have been identified that provide adequate DD and XD pointing accuracy down to point sources with a mean $F_\lambda=10^{-17}$ ergs/cm^2/s/Å. Furthermore, it has been pointed out that an iterative application of the LTAIMCAL procedure can be used to remove 1-step OSM1 rotation errors. Without this iterative LTAIMCAL procedure, there is no guarantee of meeting the ± 50 spectral resolution element alignment of the desired and achieved central wavelength for NUV observations.

If MAMA hot spots are of concern, or an algorithm is desired that can accurately center targets fainter than $F_\lambda=10^{-17}$ ergs/cm^2/s/Å, then we have identified two LTAIMAGE methods that achieve the desired accuracies. These methods are the “small box” (170x170p) STIS-like moving box plus flux-centroid (MBPFC) method and the “small box” 2-1D histogram maximum method. The MBPFC method achieves higher accuracy at the expense of increased computation time, and requires that the exposure be performed in ACCUM mode or that the TIME-TAG event list be converted into a 2-D histogram (image). The MBPFC method has the advantages of being proven in orbit and known to work on extended targets.

Caution must be exercised to not exceed the local count rate limit for the NUV MAMA. Accurate knowledge of the integrated flux from 1700-3200Å is essential for a safe and successful LTAIMAGE TA. Attenuation with the RVMM and BOA+RVMM modes allow this procedure to be used for sources over a large range of fluxes, $10^{-17} < F_\lambda < 10^{-11}$ ergs/cm^2/s/Å.

Most LTACAL+LTAIMAGE TAs should take less than 6 minutes.

NOTE: During the COWG of 1/18/01, it was agreed that the 'STIS-like' MBPFC method, using an ACCUM image that will be retained for downlink, would be recommended for flight software use. See COS-11-0014 Rev A for further details.